

UAV-Assisted Wireless Communications: An Experimental Analysis of Air-to-Ground and Ground-to-Air Channels in Open Environments

Kamran Shafafi, Eduardo Nuno Almeida, André Coelho, Helder Fontes, Manuel Ricardo, Rui Campos
INESC TEC and Faculdade de Engenharia, Universidade do Porto, Portugal
{kamran.shafafi, eduardo.n.almeida, andre.f.coelho, helder.m.fontes, manuel.ricardo, rui.l.campos}@inesctec.pt

Abstract—Unmanned Aerial Vehicles (UAVs) offer promising potential as communications node carriers, providing on-demand wireless connectivity to users. While existing literature presents various channel models, they often overlook the impact of UAV heading. This paper experimentally characterizes Air-to-Ground (A2G) and Ground-to-Air (G2A) wireless channels in obstacle-free, interference-free open environments, accounting for distance and UAV heading. We analyze the Received Signal Strength Indicator (RSSI) and TCP throughput between ground users and UAVs, covering distances between 50 m and 500 m, and considering different UAV headings. Our study offers a more accurate channel model characterization compared to deterministic models such as Friis and two-ray. Additionally, we characterize the antenna's radiation pattern based on UAV headings.

Index Terms—Wireless Channel Characterization, UAV Communications, Air-to-Ground, Ground-to-Air.

I. INTRODUCTION

Due to their decreasing cost, size, and weight, as well as their increasing battery life, high maneuverability, and ability to hover, Unmanned Aerial Vehicles (UAVs) have emerged as interesting platforms for a wide set of applications, such as surveillance, aerial imagery, operations in unreachable areas, delivery of goods, and search and rescue missions [1]. A key capability envisioned by 5G and beyond cellular networks is quickly deploying and providing on-demand temporary wireless connectivity in emergencies and crowded areas. In this regard, the use of UAVs forming aerial wireless networks has been noted as a cost-effective and flexible solution to carry the network hardware and establish a temporary network infrastructure, able to provide Internet access and enhance the capacity of existing networks [2]. Sending non-critical data, such as video transmission, requires the maximization of the throughput between the users on the ground and the UAV while tolerating errors and delays. However, sending critical data such as control signals (e.g., controlling robots for search and rescue missions, UAV controls) requires high Quality of Service (QoS), namely low delay and Packet Loss Ratio (PLR) [3]. Still, establishing wireless channels face many challenges. In this regard, Wireless channel modeling and characterization are important for designing and optimizing wireless communications systems. Accurate models allow the prediction of the signal quality, evaluate system performance, and develop new wireless technologies. They enable network



Fig. 1. ATLAS site, showing the hangar where the experimental measurements were performed.

designers to identify potential problems and optimize system parameters, making wireless channel modeling a critical area of research in the field of wireless communications. In addition to establishing a reliable link, the QoS requirements such as throughput, PLR, and delay should be considered [4]. To ensure the establishment of a reliable broadband wireless link considering the metrics mentioned above, channel modeling and measuring the channel characteristics is necessary. Several measurement methods and approaches considering different key parameters have been proposed in the literature, including modeling, statistical analysis, and experimental measurements, to characterize channels in various environments and altitudes. The antenna orientation and height of the receiver as well as the heading of the UAV can have a significant impact on the performance of the wireless channels. However, existing research mainly focuses on A2G channel modeling, with less emphasis on above mentioned parameters.

The main contribution of this paper is the experimental characterization of the A2G and G2A wireless channels in an obstacle-free, interference-free open environment. The characterization of the channel is performed at different distances and UAV headings within the context of the ResponDrone project [5]. We analyze the Received Signal Strength Indicator (RSSI) and the TCP throughput between the user on the ground and the UAV for distances ranging from 50 m to 500 m, and considering different headings of the UAV. Moreover, we provide a more accurate characterization of the channel model, when compared to deterministic models, such as Friis and two-ray. Finally, we also characterize the Effective Radiation Pattern (EDP) based on the UAV headings.

The remainder of this paper is organized as follows. The related work is presented in Section II. The system model is described in Section III. The methodology to model the experimental wireless channels is presented in Section IV. The experimental results are analyzed in Section V. Finally, Section VI draws conclusions and points out future work.

II. RELATED WORK

In the context of AG communications channel characterization for UAVs, different measurement models and approaches are presented in the literature. In [6], the authors surveyed and analyzed the A2G, G2G, and A2A channel measurements and models for both civil aeronautical and UAV communications. This paper analyses the link budget of UAV communications and presents design guidelines for managing the link budget taking account of propagation losses and link fading. In [7], the authors presented a model for the characterization of the A2G and G2A channels, while UAV was hovering at different altitudes including different Line-of-Sight (LoS) distances from the User Equipment (UE). The channel model has been analyzed in terms of path loss and fast-fading components. In [2], A2G channel measurements are presented for small-sized UAVs at different environmental conditions and altitude values between 15 and 105 m. Path loss, shadow fading, Doppler effect, Power Delay Profile (PDP), Root-Mean-Square (RMS) delay spread, RMS doppler frequency spread, and the Rician K-factor were used to characterize the channel. The Rician K-factor is one of the main characteristics of a wireless channel to define the ratio of the signal power in the LoS component to the scattered power.

In [8], the authors reviewed empirical models for the A2G and A2A propagation channels. Then it classifies the UAV channel modeling approaches as deterministic, stochastic, and geometric-stochastic models. In [9], the authors present an experimental result on how the height of the receiver affects Radio Frequency (RF) signal propagation over the sea; they concluded that it has a major impact on the present capacity and range of the radio link. In [10], the authors proposed an architecture of a new model for the A2G channel. The modeling is based on 10MHz channel-sounding flight measurements. The key advantage of the proposed A2G channel modeling approach is its flexibility to a wide range of potential ground station deployment scenarios. In [11], experimental results in different environments utilizing commercial Long-Term Evolution (LTE) deployments were conducted to evaluate the variation of the mean Angle of Arrival (AoA) and Angular Spread (AS) with flying altitude. The authors of the deployment scenarios in [11] used sixteen antennas and LTE cellular signals, to experimentally evaluate the performance of the A2G channel, taking into account the UAV altitude variation. Maximum ratio combining and conventional beamforming techniques have been compared with a single antenna system. [12], presented an experimental measurement campaign for the A2G channel at 10MHz and provided results on measured channel characterization. The desired measurements have been made with short (30 m – 330 m) and long (9 Km-11 Km)

distances between the receiver and the transmitter. In [13], measurements with a helium balloon in stationary positions at altitudes up to 500 m have been considered for the A2G channel model. The Euclidean distance between the base station and the receiver was 1900 m. The experiments have been conducted using passive sounding of UMTS and GSM signals in an urban environment at a central carrier frequency of 2120 MHz. A statistical model for AG channels in urban Environments and carrier frequency range from 200 MHz to 5 GHz was proposed in [14]. Using RSSI values, in [15], the authors calculated the path loss exponent for AG networks while the UAV was flying over both an open field and a campus area. The authors also measured the UDP throughput of the Air-Ground-Air (AGA) links.

Wireless channel modeling with the accurate characterization of the RSSI and throughput, accounting for the UAV headings, in different distances between UAVs and users, has not been addressed so far.

III. SYSTEM SETUP

The system model of this paper consists of one UAV acting as Access Point (AP) and one UE on the ground. The UAV carries a wireless communications module including a Wi-Fi interface to provide wireless connectivity to UE and a processor. Two antennas are horizontally mounted on the UAV's payload in the front, with one pointing North/South and the other East/West, considering the "North" as the head of the UAV. These antennas are omnidirectional with a gain of 5dBi and are used for the Wi-Fi link to serve the UE. Additionally, two antennas are vertically mounted in the back part of the UAV, which are omnidirectional triband antennas used for the LTE link to a remote Base Station (BS). The UE is a smartphone carried by a person, allowing to communicate with UAV.

The IEEE 802.11n (Wi-Fi 4) standard was used, with MIMO 2x2, and operating in channel 1 with a bandwidth of 20 MHz. The LTE BS was located 120 m away from the hangar as depicted in Fig. 1. This BS provides LTE coverage in Band 3 (1.8 GHz) without carrier aggregation, which leads to theoretical throughput values up to 150 Mbit/s for downlink and 50 Mbit/s for uplink. Finally, The TCP traffic flow was generated from the UAV to the Smartphone and Wi-Fi MAC auto-rate mechanism (Minstrel) was installed as a wireless link adaption.

IV. FIELD TRIAL

The experimental measurements will provide valuable insights into the wireless communication system's behavior, helping to identify potential areas for improvement and optimize the system design for better efficiency and reliability. The experimental plan of this paper is aim at conducting experiments in a real-world scenario to evaluate the wireless communications system's performance by means of an experimental measurement testbed. The wireless channel performance between the UAV and the UE is characterized in terms of RSSI and throughput measured at each antenna,

considering different UAV headings and distances, which are key parameters for evaluating wireless communication systems. The experimental measurements are represented in separate plots and compared with theoretical models, such as Friis and two-ray ground-reflection models. In this section, the experimental scenarios and setup are presented.

A. Experimental Scenarios

Three scenarios are evaluated in what follows:

1) *Scenario A*: In this experiment the UAV was positioned 200 m away from the UE (horizontal distance), flying at 50 m Altitude above Ground Level (AGL). The Euclidean distance between UE and UAV was 206 m. The UAV was rotated in incremental steps of 45° until it made a full turn. This experiment was performed to measure the Effective Radiation Pattern (ERP) of the antennas, since the UAV's body changes this pattern by obstructing and reflecting the signal, depending on the relative heading between the UAV and the UE. The RSSI is measured (in dBm) from the packets received by the antennas and depicted in the same figure with the Friis model for a better understanding and comparison. Also, downlink throughput is measured at the UE (in Mbit/s) in various headings of UAVs.

2) *Scenario B*: In this experiment, we moved the UAV away from the UE in a step of 25 m, while maintaining the UAV at 50 m AGL, with a heading of 180° relative to the UE. The UAV then comes back towards the UE, repeating the same waypoints as before, but with an opposite heading (0°). During this experiment, the RSSI measured at UAV and the downlink throughput measured at UE is evaluated. The RSSI was compared with Friis and two-ray ground-reflection models.

3) *Scenario C*: In this test, the UAV was located at 1.42 Km away from the LTE BS. We measured the Internet throughput achieved when the UE is directly connected to the LTE BS compared to when the UE is connected to the LTE BS through the UAV using Wi-Fi.

B. Experimental Setup

A payload, depicted in Fig. 2, is installed in an Alpha 800 UAV, and acts as a flying AP, to which UE can access the Internet. It comprises an APU 4D4 board, a processor with quad cores of 64-bit/1 GHz, which is paired with 4 GB of RAM, the OpenWRT 19.07.8 operating system, an M. SATA 32GB solid-state drive (SSD), and 16GB of SD memory. A throughput test was performed near the hangar (using an LTE UE), through which we could confirm that a network throughput close to the theoretical limits of the technology could be achieved as can be seen in Fig. 3 (114 Mbit/s for downlink and 55 Mbit/s). The link quality degrades with the distance due to signal propagation loss, but this BS is enough to provide sufficient cellular coverage up to 1km around the hangar. At 1.2 Km away from the hangar we measured the LTE throughputs of around 11 Mbit/s for downlink and 1 Mbit/s for uplink.



Fig. 2. Communications payload installed in the ALPHA 800 UAV.

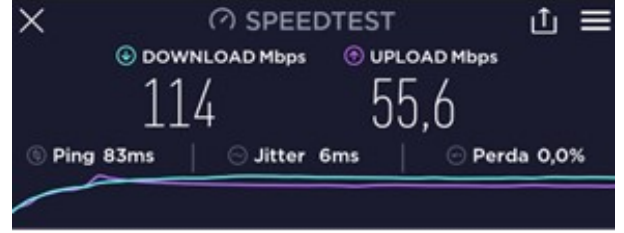


Fig. 3. LTE throughput test result near the hangar measured at the LTE UE.

To generate enough traffic to saturate the Wi-Fi link and assess its performance, we used an iperf3 TCP server installed on the FAP. The traffic flow was generated from the FAP to the Smartphone and installed tcpdump on the UAV to measure RSSI on antennas. A Xiaomi Mi 9T Android smartphone was used as UE and this smartphone was selected with single antenna capability as the worst-case scenario. If a smartphone with MIMO (2 antennas or more) is used, better network performance should be experienced than the baseline we are assessing here. We used an iperf3 client application on the smartphone to monitor the throughput.

V. EXPERIMENTAL RESULTS

This section shows the results of the three experimental measurement scenarios.

A. Scenario A: Received Signal Strength and Throughput vs. UAV heading

Fig. 4 presents the ERP of each antenna by measuring RSSI from the packets received by the antennas. The 1st Antenna (red color) represents the antenna oriented North/South, and 2nd Antenna (blue color) represents the antenna positioned East/West. The orange line represents the RSSI of the Friis theoretical model, considering an isotropic antenna, and was drawn only as a reference to the peak RSSI expected for each antenna when aligned with the direction of maximum gain. As can be seen, because of the misalignment the orientation of the antennas the radiation pattern in the East-West direction for the red antenna as well as in the North-south direction for the blue antenna is so different from Friis models. If the summation of both antennas is considered this issue will be solved.

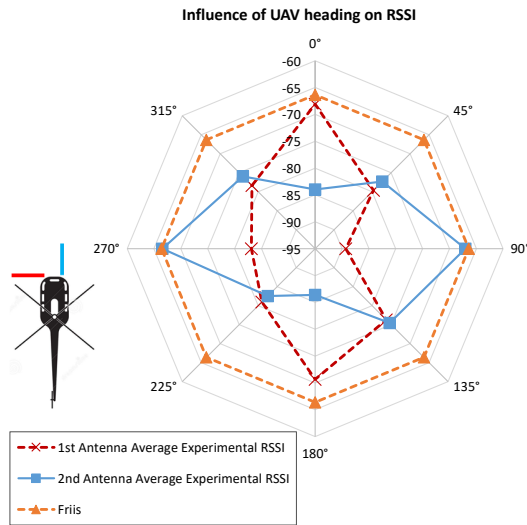


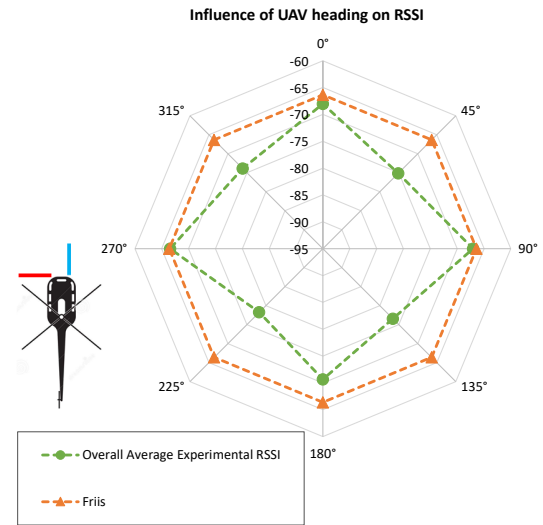
Fig. 4. Scenario A – Effective radiation pattern of the 1st antenna (red) and the 2nd antenna (blue) by measuring the RSSI from the packets received by the antennas on the UAV and comparing with the Friis baseline.

Fig. 5a, shows the effective resulting RSSI for one spatial stream when summing the signal received in both antennas. In Fig. 5b, the achievable downlink throughput for the same UAV headings is depicted. The presented values depict the best and worst-case scenarios, showing that the throughput can vary from approximately 30 Mbit/s (N, S, E, and W) to approximately 10 Mbit/s (NE, SE, SW, and NW). Since the used antennas are omnidirectional, it would be possible to have the same received power level independently of the UAV heading, as depicted by the orange line for Friis. However, in real-world experiments, the antennas have a heterogeneous radiation pattern; this can be concluded by different received power levels for different headings. In general, the relationship between RSSI and throughput is complex and depends on various factors such as the signal-to-noise ratio, modulation scheme, and channel conditions. A high RSSI does not necessarily imply a high throughput and vice-versa. For example, a strong signal may still experience a high level of interference, which can reduce the throughput. However, in this paper, if comparing Fig. 5a and Fig. 5b because of the lack of obstacle and interference in the scenario, can be drawn that high RSSI results in high throughput and vice-versa. Additionally, from Fig. 5a, can be drawn that at 180° the RSSI is lower than expected. It is due to the obstruction of the UAV's body.

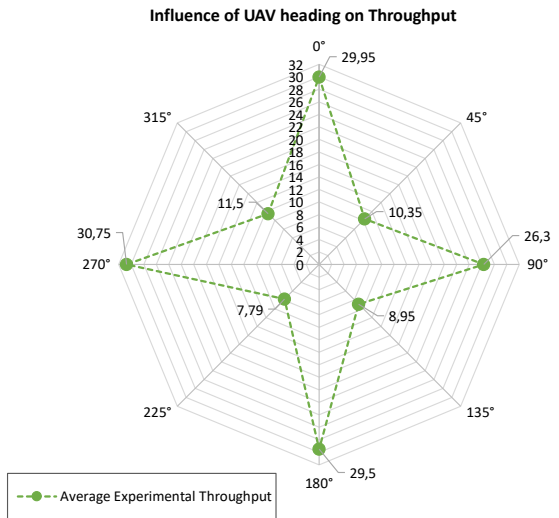
Fig. 6, represents the resulting expected Coverage for -85 dBm of RSSI (link still stable but low throughput) and -75 dBm (link with still good performance for multiple video streams) cut-offs. During the tests, we were able to have Internet connectivity beyond 1.5 Km (the UE remained connected, and browsing the Internet was still possible).

B. Received Signal Strength and Throughput vs. Distance

Fig. 7a, depicts the experimental RSSI results compared with the Friis and two-ray ground reflection propagation loss



(a) Effective resulting RSSI for one spatial stream when summing the signal received in both antennas, comparison with the Friis baseline.



(b) Achievable downlink throughput for the same UAV headings measured at UE.

Fig. 5. Scenario A – Effective radiation pattern by measuring total RSSI (sum of two antennas) on UAV, and downlink throughput measured on the UE.

models as well as the downlink throughput when the UAV moves away from the UE, and Fig. 7b, shows these parameters when the UAV comes back toward UE.

Due to obstruction of the UAV's body, as expected the RSSI was lower when the UAV moved away (180° heading) than when coming back to the UE (0° heading). The lower throughput values when coming back are related to a limitation of the Minstrel, which is known to delay the increase of the data rate when the link conditions improve in a short period of time. That is why when the UAV was refueled at a specific distance (Fig. 7a at 130 m) and the speed test at the same exact coordinates is redone as before, the throughput is improved (to speeds equivalent to the ones obtained when the

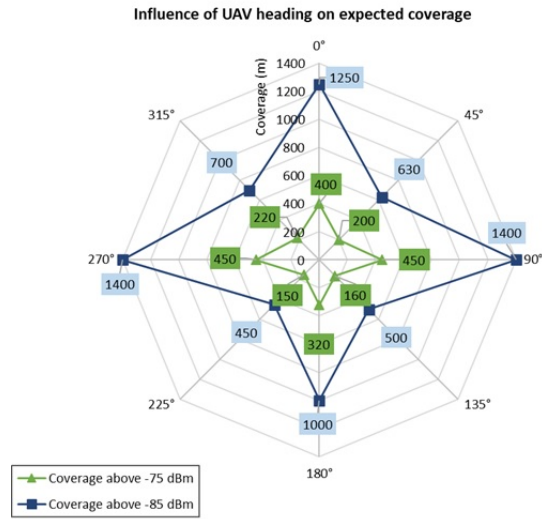


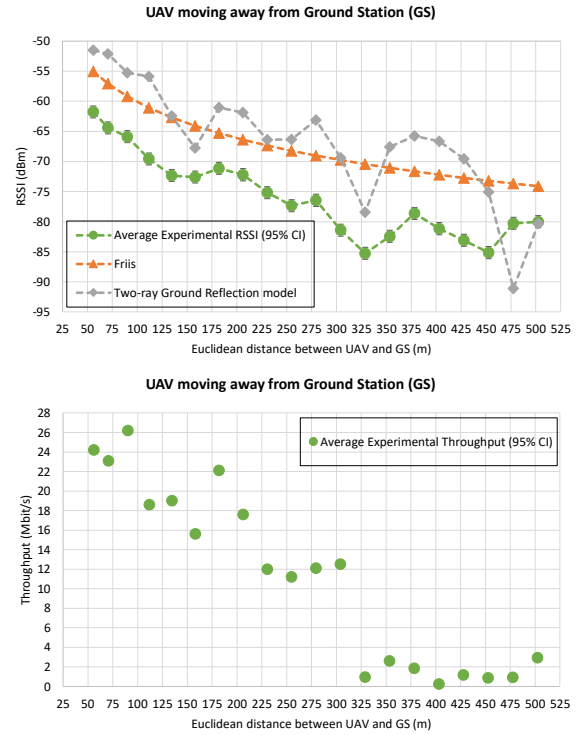
Fig. 6. Scenario A – Resulting expected coverage for -85 dBm (link still stable but low throughput) and -75 dBm (link with still good performance for multiple video streams) cut-offs.

UAV was moving away from the user). Sometimes, restarting the Wi-Fi card was needed to clear the Minstrel history so that an optimal rate was found faster. Additionally, when moving away from the UE, the steep decline in throughput is caused by link asymmetry of link (10 dB). That is, the MAC acknowledgments (ACKs) are sent at 24 Mbit/s whenever the data packets are received at 24 Mbit/s or above (fast ACK mechanism). Even though from A2G there is a good SNR to use higher Modulation Code Schemes (MCSs), it comes at a time when the G2A SNR is too low to allow successful acknowledgments at 24 Mbit/s. When it happens, the data packets are "forced" to be sent at lower MCSs so that the ACKs are generated below 24 Mbit/s.

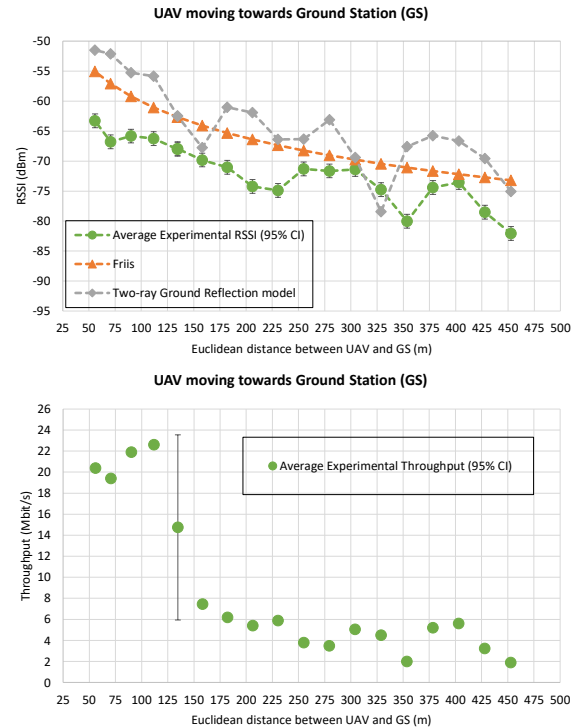
In terms of the coverage and throughput significant results were achieved as depicted in Fig. 8. For the green area, the throughput was between 10 Mbit/s and 80 Mbit/s, and the coverage for N, S, E, and W directions had a radius of 400 m for cell phones with a single antenna. Coverage in NE, SE, SW, and NW directions was a radius of 200 m for cell phones with a single antenna. For the blue area, the throughput was more than 1 Mbit/s, and the coverage for N, S, E, and W directions was the radius of 1100 m for cell phones with a single antenna. Coverage in NE, SE, SW, and NW directions was a radius of 550 m for cell phones with a single antenna. We had a coverage radius of 1500 m successful experiment by a cell phone with two antennas.

C. Scenario C: Internet Access vs LoS

As depicted in Fig. 9, while the UE was connected via LTE, the UE achieved up to 13 Mbit/s; when the UE was connected through the UAV it reached up to 21 Mbit/s at the same location, representing a gain of 1.6x. The terrain topography and existing trees were blocking the radio line-of-sight (LoS) between the UE and the LTE BS, while through



(a) UAV moving away from UE in steps of 25 m, while maintaining a flight at 50 m AGL.



(b) UAV comes back towards the UE, repeating the same waypoints as before.

Fig. 7. Scenario B – Experimental RSSI measured on UAV compared with the Friis and two-ray ground baselines and the downlink throughput measures on UE when UAV moving away from the UE and vice-versa.

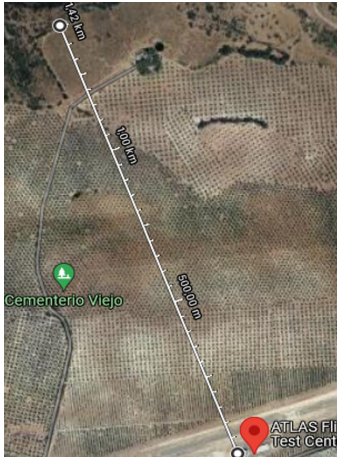


Fig. 8. Coverage and throughput we achieved in this paper that has divided into two main green and blue regions.

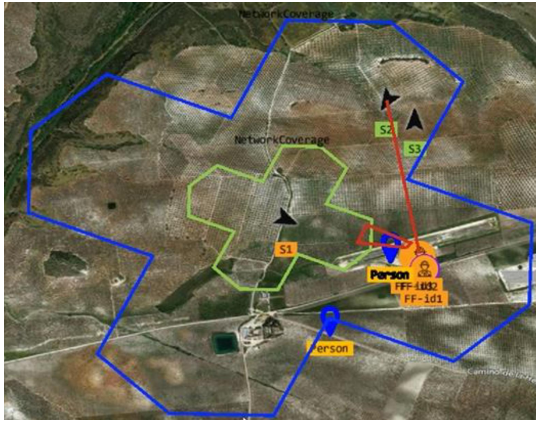


Fig. 9. Scenario C - Distance of the UE to the hanger. UE connected via LTE and via FAP at the same location.

the FAP those obstacles were circumvented and radio LoS was ensured.

VI. CONCLUSIONS

In this work, a successful internet connection between a UAV and a UE was tested at a distance of up to 1500 m, and the performance, given that the cell phone is the "weakest link" (has internal antennas and lower power). We found that the antennas in real-world experiments can have a heterogeneous radiation pattern; this can be concluded by scenario A. Due to the obstruction of the UAV's body at 180°, the RSSI is lower than expected. In this study, we successfully demonstrated the potential of UAVs for providing wireless connectivity between the UAV and the UE over significant distances. Our experiments revealed that real-world antenna radiation patterns can be heterogeneous, and the impact of the UAV's body and heading on signal strength should be considered when designing airborne communications systems. We found that UEs with different antenna configurations can affect the connectivity range with the UAV, emphasizing the importance of optimizing antenna design for UAV communica-

tions systems. Furthermore, our findings showed that the RSSI was generally lower when the UAV moved away from the user compared to when it returned, highlighting the need for further investigation into the effects of UAV motion on signal strength. This study offers valuable insights into the potential of UAVs for providing wireless connectivity and the importance of considering UAV heading and antenna configurations in real-world scenarios. Our findings may be valuable for future research and development of UAV communication systems and contribute to the optimization of wireless connectivity in various applications.

REFERENCES

- [1] Y. Zeng, R. Zhang, and T. J. Lim, "Wireless communications with unmanned aerial vehicles: Opportunities and challenges," *IEEE Communications Magazine*, vol. 54, no. 5, pp. 36–42, 2016.
- [2] J. Rodríguez-Piñero, T. Domínguez-Bolaño, X. Cai, Z. Huang, and X. Yin, "Air-to-ground channel characterization for low-height uavs in realistic network deployments," *IEEE Transactions on Antennas and Propagation*, vol. 69, no. 2, pp. 992–1006, 2021.
- [3] E. Yanmaz, R. Kuschig, and C. Bettstetter, "Achieving air-ground communications in 802.11 networks with three-dimensional aerial mobility," in *2013 Proceedings IEEE INFOCOM*. IEEE, 2013, pp. 120–124.
- [4] —, "Channel measurements over 802.11 a-based uav-to-ground links," in *2011 IEEE GLOBECOM Workshops (GC Wkshps)*. IEEE, 2011, pp. 1280–1284.
- [5] M. Friedrich, T. J. Lieb, A. Temme, E. N. Almeida, A. Coelho, and H. Fontes, "Respondrhone-a situation awareness platform for first responders," in *2022 IEEE/AIAA 41st Digital Avionics Systems Conference (DASC)*. IEEE, 2022, pp. 1–7.
- [6] C. Yan, L. Fu, J. Zhang, and J. Wang, "A comprehensive survey on uav communication channel modeling," *IEEE Access*, vol. 7, pp. 107 769–107 792, 2019.
- [7] E. N. Almeida, A. Coelho, J. Ruela, R. Campos, and M. Ricardo, "Joint traffic-aware uav placement and predictive routing for aerial networks," *Ad Hoc Networks*, vol. 118, p. 102525, 2021.
- [8] A. A. Khuwaja, Y. Chen, N. Zhao, M.-S. Alouini, and P. Dobbins, "A survey of channel modeling for uav communications," *IEEE Communications Surveys & Tutorials*, vol. 20, no. 4, pp. 2804–2821, 2018.
- [9] F. B. Teixeira, R. Campos, and M. Ricardo, "Height optimization in aerial networks for enhanced broadband communications at sea," *IEEE Access*, vol. 8, pp. 28 311–28 323, 2020.
- [10] N. Schneckenburger, T. Jost, U.-C. Fiebig, G. Del Galdo, H. Jamal, D. Matolak, and R. Sun, "Modeling the air-ground multipath channel," in *2017 11th European Conference on Antennas and Propagation (EuCAP)*, 2017, pp. 1434–1438.
- [11] T. Izydorczyk, F. M. Tavares, G. Berardinelli, M. Bucur, and P. Mogensen, "Angular distribution of cellular signals for uavs in urban and rural scenarios," in *2019 13th European Conference on Antennas and Propagation (EuCAP)*. IEEE, 2019, pp. 1–5.
- [12] N. Schneckenburger, D. Shutin, T. Jost, M. Walter, T. Thiasiriphet, A. Filip, and M. Schnell, "From l-band measurements to a preliminary channel model for apnt," in *Proceedings of the 27th International Technical Meeting of the Satellite Division of The Institute of Navigation (ION GNSS+ 2014)*, 2014, pp. 3009–3015.
- [13] N. Goddemeier, K. Daniel, and C. Wietfeld, "Role-based connectivity management with realistic air-to-ground channels for cooperative uavs," *IEEE Journal on Selected Areas in Communications*, vol. 30, no. 5, pp. 951–963, 2012.
- [14] Q. Feng, J. McGeehan, E. K. Tameh, and A. R. Nix, "Path loss models for air-to-ground radio channels in urban environments," in *2006 IEEE 63rd vehicular technology conference*, vol. 6. IEEE, 2006, pp. 2901–2905.
- [15] E. Yanmaz, R. Kuschig, and C. Bettstetter, "Channel measurements over 802.11 a-based uav-to-ground links," in *2011 IEEE GLOBECOM Workshops (GC Wkshps)*. IEEE, 2011, pp. 1280–1284.